Three-dimensional Superposition of Diffuse Optical Tomography Results and Subjacent Anatomic Structures

Christina Habermehl[1], Christoph Schmitz[1,2], Jan Mehnert[1,3], Susanne Holtze[1,3], Jens Steinbrink[1,4]
[1]Berlin NeuroImaging Center,Charité Dept. of Neurology, Charitépl. 1, 10117 Berlin, Germany,
[2] NIRx Medizintechnik GmbH, Berlin, Baumbachstr. 17, 13189 Berlin, Germany,
[3]Max Planck Institute for Human Cognitive and Brain Sciences, Stephanstr. 1a, 04103 Leipzig, Germany,
[4]Center for Strokeresearch Berlin (CSB), Charité Universitätsmedizin, 10098 Berlin, Germany

ABSTRACT

Near infrared spectroscopy (NIRS) and diffuse optical tomography (DOT) reveal no information about the measurement's underlying anatomical structures. An independent anatomical mapping of DOT results onto the subject's brain or a generic brain model is desirable, especially when regions prone to large inter-subject variability are studied. We show two methods to match DOT data from high density fiber grids to anatomical structures. The forward model that is used to predict the light propagation is based on one generic anatomical MR scan. In both approaches we use this model MR-scan to translocate the position of the optical fiber grid from our experimental setup to the FEM model space. The fiducial mark approach uses the spatial normalization of the subject's MR-scan (with marked corners of the fiber grid) and the model's MR scan, leading to a translocation of the fiber pad position to the FEM-Model space. The anatomic landmark approach is used without individual MR scan. 19 reference points and the position of the fiber pad corners are determined using photogrammetry software. These coordinates are translocated to the FEM model space by solving the least square problem of the subject's and the model's reference points. We illustrate and compare both methods and show results from a vibrotactile stimulation experiment in humans.

Keywords: near infrared spectroscopy, diffuse optical tomography, anatomical mapping, human brain function

1. INTRODUCTION

Non-invasive NIRS is an established tool for revealing cortical activation through changes in the degree of hemoglobin oxygenation in the activated area. Near infrared light is given into the subject's brain by optical fibers, which are placed on the head surface. Differences in the light attenuation are then used to calculate interiour absorption changes that are mainly caused by a cortical activation and a locally increased blood flow.

The topographic approach in NIRS, uses data from next nearest neighbours with source-detector-distances of 2-4cm. This method is an established tool in phyiological and psychological research [1-3] and it is known to have a good temporal but a rather poor lateral resolution.

The lateral resolution can be enhanced by a multi-distance approach [4, 5]. Arrays of closely spaced fibers allow the simultaneous measurement of light paths from different tissue depths. These overlapping photon paths and an image reonstruction procedure lead to a series of three-dimensional reconstructed images of changes of interiour optical properties. This optical tomography approach has a rough depth discrimination and facilitates the separation of signals from superficial and deeper layers.

The image reconstrution procedure for 3D DOT contains of two major steps. First, the light propagation in the medium with asumed optical properties is modeled. This leads to a sensitivity matrix that contains information about the contribution of each voxel in the medium to the measured surface data. Secondly, the inverse problem of recovering interior optical properties from the surface data is solved, mainly by multiplying the inverted sensitivity matrix and the detected light intensity values from the surface. Image reconstruction is an ill-posed and under-determined problem and many groups work on one or both parts of it [5-11].

As topographic NIRS and 3D DOT itselves reveal no information about underlying anatomical structures, a co-registration of the optical fiber positions and the forward model geometry is needed to subsequently map the results onto anatomical structures like individual MR scans or the scan of a generic atlas. This mapping is often desired, especially when regions are studied that are known for a large inter-subject variability concerning location and extend of the activation patterns.

In this work we present two methods to co-register optical probe positions from the real world space (subject's head surface) with the finite element (FE) head geometry that is used to calculate the forward model. We used the same generic FE-model for all subjects. However, after co-registration, the probe positions on the forward model were individually determined for every subject.

First we show a fiducial mark approach using individual anatomic MR scans of each subject with marked fiber grid positions on the head surface. Secondly we present an anatomic landmark approach for cases when a subject's MR scan is not available. Both methods allow the mapping of the three-dimensional reconstruction result volumes onto anatomical structures. Using the first method, the results can be mapped onto individual brain structures, for the second approach the results are mapped onto a generic brain atlas.

2. METHODS

2.1 Subjects, stimulus procedure and optical data acquisition

We investigated eight healthy voluntary subjects (mean age 26.8 ± 4.6 years, 2 female) with approval by the local ethics committee at Charité University Hospital Berlin and written consent from each subject prior to the experiment.

All subjects were stimulated vibrotactily at the 1st and 5th finger of the right hand in pseudo randomized order (20s stimulation followed by 20s rest, 40 repetitions per finger) using a piezoelectric transducer (model PL-127.251, PI Ceramic, Lederhose, Germany) with a flat semicircle-shaped rubber pad (diameter, 13 mm) on the top surface, vibrating with a rate of 40 Hz (Figure 1a). The transducer was gently fixed at the subject's fingertips with adhesive tape to assure the correct position throughout the whole experiment.

Neural activity was measured with a rectangular grid (3.0 x 3.75 cm) of 30 optical fibers over the contralateral peri-central area. Each fiber served as source and detector facilitating the acquisition of 900 simultaneous optical data channels using the DYNOT 232 optical tomography imager (NIRx Medizintechnik GmbH, Berlin, Germany). The system performs continuous-wave measurements using two laser sources of 760 nm and 830 nm in a time-multiplexed scanning fashion at a sampling rate of 1.8Hz. Details of the imaging device can be found in [12].

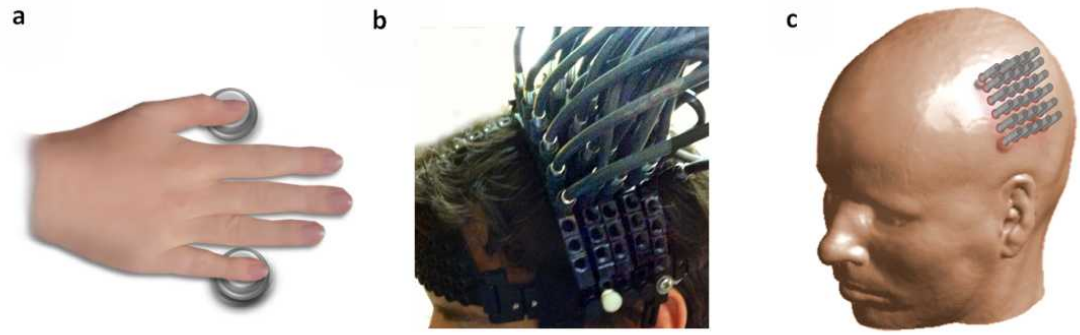

Figure 1 Experimental setup. Vibrating piezoelectric transducers were fixated on the first and the fifth finger of the right hand. Stimulation of the fingers alternated pseudo-randomly with 40 repetitions of 20 sec duration for each condition. b) 30 optical fibers (inter-optode distance 0.75 cm, six rows with 5 fibers) were placed over C3. c) Schematic image of optical probe setup.

2.2 Forward model

To generate the forward model, we used the BrainModeler software (*NIRx* Medical Technology Llc, Glen Head, NY, USA) that runs in a MATLAB (The MathWorks, Natick, MA, USA) environment. The software contains a library of overlapping FE meshes with precalculated forward solutions of the photon diffusion equation and reference detector values with assumed homogenous interior optical properties (μ_a= 0.06 cm^{-1}, μ_s= 10 cm^{-1}) considering only absorption related changes for wavelengths of 760 and 830 nm. These meshes are based on a single-subject head atlas, obtained by an anatomical MR scan with 1mm resolution.

For each subject we assigned the positions of the optical fibers to the FE-mesh individually. We present two methods to translocate the optical probe position from the subject's head surface in the real world space to the correct position on the FE-model geometry in the reconstruction space.

2.3 Fiducial mark approach

For the first method, prior to the optical data acquisition, we indicated the corner positions of the imaging grid with oil-filed capsules (Vitamin E AL 400, Aliud Pharma GmbH, Laichingen, Germany), serving as fiducial marks and giving a good contrast in T1 weighted MR images. Subsequently, we acquired an anatomical T1-weighted MPRAGE (TR=94 ms, TE=4 ms, flip angle 12°, voxel size 1 mm x 1 mm x1 mm) MRI scan (1.5 T, Magnetom Vision, Siemens, Erlangen, Germany) for every subject (Figure 2a). We then co-registered the subject's anatomic scan with the MR scan of the generic head model (Figure 2b). This MR scan was originally used to create the FE-model geometry and both are located in the same space.

Using the spatial preprocessing tool from SPM8 (The Wellcome Trust Centre for Neuroimaging, University College London, http://www.fil.ion.ucl.ac.uk/spm), we normalized the subject's MR scans with the MR scan of the head model. We defined the subject's scan as source image and the head model as the template. The SPM8 spatial normalization tool computes an affine and subsequently a non-linear transformation between the two volumes. The source image was warped to fit into the boundaries of the template image without losing structural information [13]. This resulted in a translocation of the subject's head to the FE-model space. Figure 2c shows one example of the warped anatomy from one subject in the FE-model space. The postions of the 30 optical fibers were interpolated between the coordinates of the fiducials and assigned to the FE-model boundary.

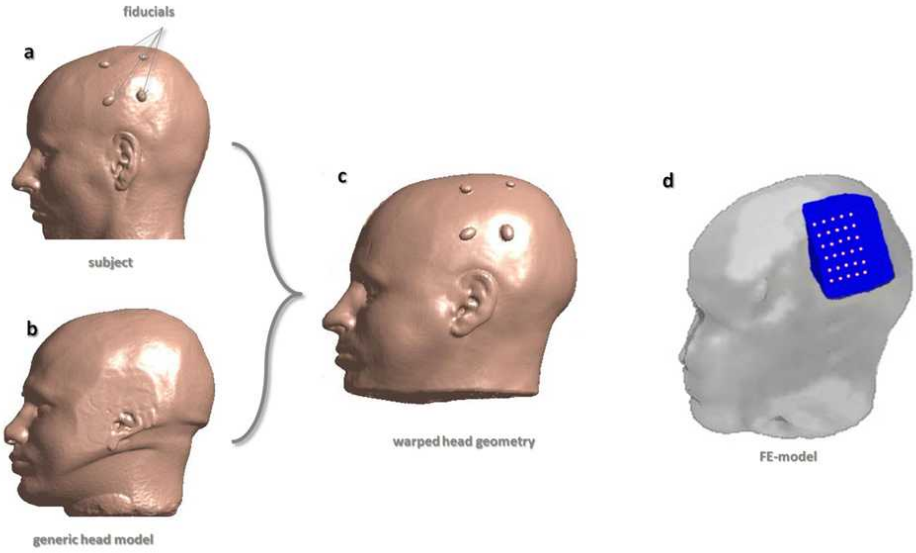

Figure 2 Fiducial mark approach; transformation of the imaging grid corner positions obtained from individual MR scan to the FEM model space. a) T1 weighted MR-scan of one subject. Corner positions of the probe pad indicated by four spheres. b) MR-scan of the generic brain model. This c) Subject's MR image after a spatial normalization (warping) to the generic brain model geometry. d) The positions of 30 optical fibers were interpolated between the fiducials and assigned to the FE-model boundary.

2.4 Anatomic landmark approach

In many studies it is not feasible to gain anatomic MR scans of every subject. The second method requires no structural scan, since the generic head atlas can be used for mapping. Coordinates of 19 reference points (from the International 10-20 system [14]) and of the 4 corner positions of the optode pad on the subjects head surface were recorded using a photogrammetric software (PhotoModeler, Eos Systems Inc., Vancouver, Canada). These fiber pad coordinates were transformed to the FEM model space by solving the least square problem (Figure 3c) of the subject's reference points (Figure 3a) and the model's reference points (Figure 3b) with an approach containing translation, rotation and scaling [15]. We then translocated the fiber positions onto the FEM mesh (Figure 3e), thereby ensuring the correct position of the reconstructed volumetric images.

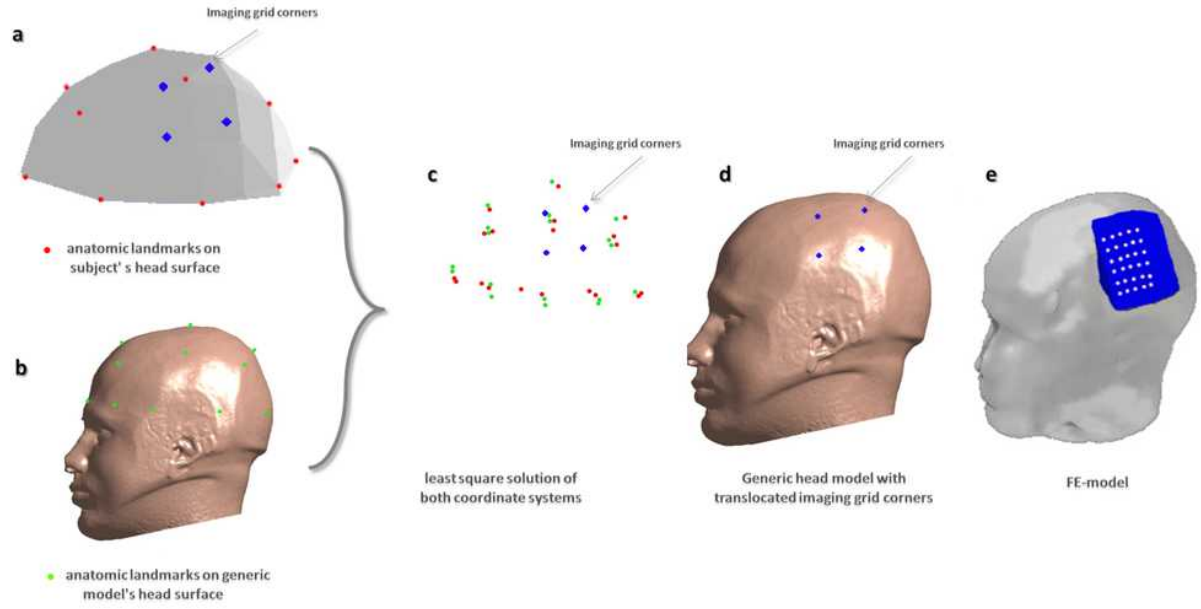

Figure 3 Anatomic landmark approach: Transformation of the optical fiber pad corner positions to the FEM model space without individual MR scan. a) 19 reference points (red dots) and coordinates of the fiber pad corners (blue dots) were acquired from the subject's head surface. b) MR scan of the generic model with 19 marked reference points (green dots) derived by [16]. c) Solving the least square problem of the two coordinate systems d) The coordinates of the grid corners are now in the generic model space, the positions (blue dots) are mapped onto the model's head surface. e) The positions of the optical probes are interpolated are and determined on the FEM model.

2.5 Image reconstruction

Raw data were band-pass filtered (0.016 - 0.4Hz) to reduce slow fluctuations, heart beat, and breathing. An image series of hemodynamic changes was reconstructed using the normalized difference method [11]. The reconstruction algorithm applies a linear perturbation equation together with a correction factor whose value is a function of accuracy of the selected reference medium. The algorithm has been shown to be robust to inaccuracies of the initial guess when relative changes of parameters are examined.

After reconstruction, we determined voxels that showed the known hemodynamic response with a decrease of HbR by calculating a paired two-tailed t-test between baseline interval (-10 to -1s before stimulus onset) and stimulus interval (13-20s after stimulus onset). We defined arbitrary cutoff values in a range of 70-90% of the minimum T-value for each subject and stimulus. Since an decrease of HbR after 5-7 sec after stimulus onset is an reliable indicator of cortical activation [17] we focused on changes in HbR rather than in HbO changes, since it has been shown that HbO is confounded by superficial tissue signaling such as blood pressure [18].

3. RESULTS

The (negative) t-values for both stimuli, indicating a strong decrease of HbR compared to the baseline were individually thresholded for each subject and condition. Voxels below this threshold were taken to mark the activation map. For the somatotopic stimulation experiment, we received two distinct activation patterns for both finger stimulations in five out of eight subjects.

Figure 4 shows the activation patterns for HbR for one subject. We present the results for both approaches. The left image displays the activation pattern, obtained with the fiducial mark approach, mapped onto the individual brain. The right images in Figure 4 shows the result obtained with the anatomic landmark approach, mapped onto the brain of the generic head model. For both methods we see the location of the activation clusters posterior to the central sulcus and in good agreement to the known somatotopic finger representation with the first finger anterior and inferior to the fifth finger [19-22]. Due to the slight difference in the optode position (mean lateral difference (y-direction) in this subject was 5mm) the results for both approaches are rather similar.

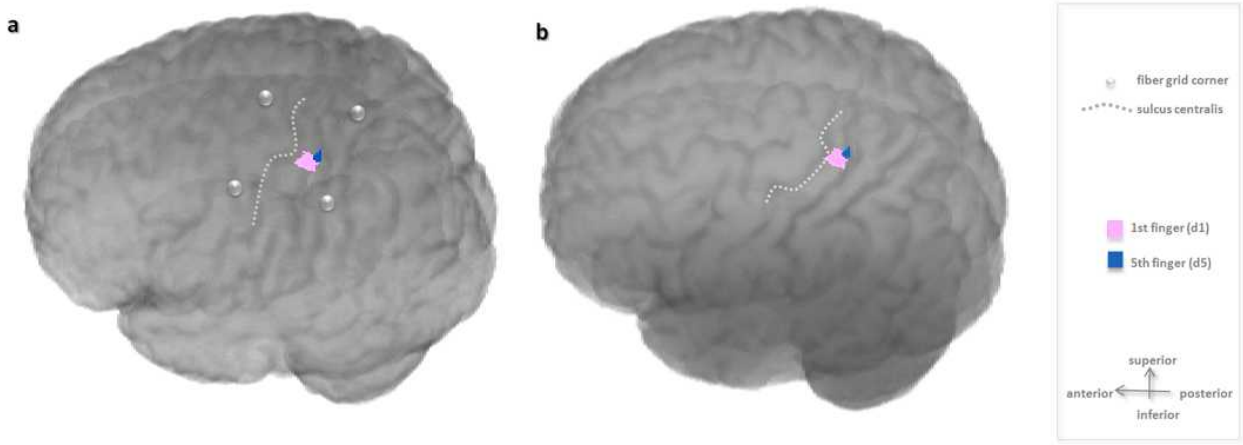

Figure 4 Results for vibrotactile stimulation of the 1st (pink) and 5th finger (blue) of the right hand. T-Values: -2.5 for the 1st finger and -3 for 5th finger for HbR. a) Optical probe positions were determined with the fiducial mark approach and results are mapped onto the subject's brain scan. b) Results for the same subject. The positions of the optical probes were determined with the anatomic landmark approach and results were mapped onto the generic head atlas. Both activation patterns are located posterior to the central sulcus (white dashed line) with a distance of their centers of about 1cm.

To determine the accuracy of the anatomic landmark approach compared to the fiducial mark approach, we calculated the difference of the fiber pad coordinates. The mean distance in y-direction was 0.49 cm ± 0.34 cm, in z-direction 0.6 cm ± 0.6 cm. We observed that subjects with larger heads showed bigger differences in the determined coordinates and that coordinates from the anatomic landmark approach were mostly positioned anterior to the fiducial marks. This can be explained by the setup procedure during which the optical fibers show a tendency to slip somewhat due to their weight and subject's movements. As a remedy, we suggest determining the location of the optical fiber positions after the experiment.

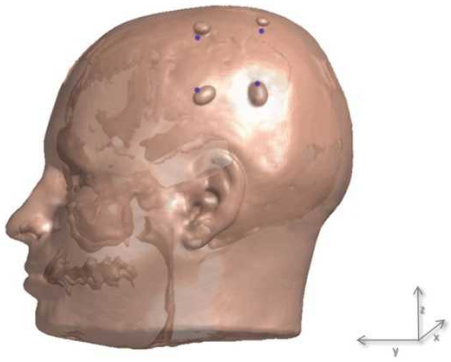

Figure 5 Comparison of the two co-registration methods. Blue dots show the positions of the optode pad corners that were determined with the anatomical landmark approach. The four spheres indicate the fiducial marks. In this case the mean difference of all four corresponding coordinate pairs was 0.14 cm ± 0.17 cm in y-direction and 0.5 cm ± 0.4 cm in z-direction.

4. DISCUSSION

NIRS and diffuse optical tomography have access to cortical activation but cannot resolve underlying anatomical structures. However, a mapping of DOT results onto an individual brain or a generic atlas is often desirable when tasks or stimuli are investigated that are known for a higher intersubject variability or when a multisubject analysis is needed.

For optical topography a method to register NIRS probe positions to the MNI space using the subject's anatomic landmarks as reference points has been proposed by [23]. Recently it has been shown for DOT [24] that using these landmarks and brain atlas for forward calculation can lead to the reconstruction of a motor activation in the correct gyrus.

In this work, we applied the anatomic landmark approach, to register the position of a high density fiber grid to the generic head atlas on which our forward geometry is based. We compared this approach with the results obtained by a fiducial mark approach, which gives direct access to the probe position on the subject's head surface. The estimated difference of the determined probe positions indicates a sufficient accuracy for the anatomic landmark approach.

We determined the position of the fiber grid with both methods and mapped the particular reconstructed volumes of a vibrotactile finger stimulation task onto the individual brain and a generic atlas. For both methods, our findings are in good agreement with the known somatotopic finger representation in the primary somatosensory cortex, postlateral to the central sulcus.

In both methods, we translocated the probe positions to the FE-model space. This allowed us the use of a generic, pre-calculated light propagation model while the individual probe positions were regarded for each subject. This is time- and energy saving compared to the generation of individual FE-mesh geometries and forward models, especially for studies comprising many subjects and using high density grids with many sources and detectors.

Acknowledgements

This work was supported in part under NIH Grant Nos.R42NS050007 and R44NS049734.

References

[1] M. A. Franceschini, D. K. Joseph, T. J. Huppert *et al.*, "Diffuse optical imaging of the whole head," J Biomed Opt, 11(5), 054007 (2006).

[2] H. Obrig, S. Rossi, S. Telkemeyer *et al.*, "From acoustic segmentation to language processing: evidence from optical imaging," Front Neuroenergetics, 2, (2010).

[3] I. Wartenburger, J. Steinbrink, S. Telkemeyer *et al.*, "The processing of prosody: Evidence of interhemispheric specialization at the age of four," Neuroimage, 34(1), 416-25 (2007).

[4] R. L. Barbour, H. L. Graber, Y. Pei *et al.*, "Optical tomographic imaging of dynamic features of dense-scattering media," J Opt Soc Am A Opt Image Sci Vis, 18(12), 3018-36 (2001).
[5] D. A. Boas, K. Chen, D. Grebert *et al.*, "Improving the diffuse optical imaging spatial resolution of the cerebral hemodynamic response to brain activation in humans," Opt Lett, 29(13), 1506-8 (2004).
[6] S. R. Arridge, and J. C. Hebden, "Optical imaging in medicine: II. Modelling and reconstruction," Phys Med Biol, 42(5), 841-53 (1997).
[7] H. Dehghani, M. E. Eames, P. K. Yalavarthy *et al.*, "Near infrared optical tomography using NIRFAST: Algorithm for numerical model and image reconstruction," Commun Numer Methods Eng, 25(6), 711-732 (2008).
[8] Q. Fang, "Mesh-based Monte Carlo method using fast ray-tracing in Plucker coordinates," Biomed Opt Express, 1(1), 165-175 (2010).
[9] Q. Fang, and D. A. Boas, "Monte Carlo simulation of photon migration in 3D turbid media accelerated by graphics processing units," Opt Express, 17(22), 20178-90 (2009).
[10] A. Gibson, and H. Dehghani, "Diffuse optical imaging," Philos Transact A Math Phys Eng Sci, 367(1900), 3055-72 (2009).
[11] Y. Pei, H. L. Graber, and R. L. Barbour, "Influence of Systematic Errors in Reference States on Image Quality and on Stability of Derived Information for dc Optical Imaging," Appl Opt, 40(31), 5755-69 (2001).
[12] C. H. Schmitz, M. Löcker, J. M. Lasker *et al.*, "Instrumentation for fast functional optical tomography," Review of Scientific Intruments, 73(2), 429-439 (2002).
[13] J. Ashburner, G. Barnes, C. Chen *et al.*, [SPM8 Manual], London, UK(2011).
[14] G. H. Klem, H. O. Luders, H. H. Jasper *et al.*, "The ten-twenty electrode system of the International Federation. The International Federation of Clinical Neurophysiology," Electroencephalogr Clin Neurophysiol Suppl, 52, 3-6 (1999).
[15] B. K. P. Horn, "Closed-form solution of absolute orientation using unit quaternions," J. Opt. Soc. Am. A, 4(4), 629-642 (1987).
[16] V. Jurcak, M. Okamoto, A. Singh *et al.*, "Virtual 10-20 measurement on MR images for inter-modal linking of transcranial and tomographic neuroimaging methods," Neuroimage, 26(4), 1184-92 (2005).
[17] H. Obrig, and A. Villringer, "Beyond the visible--imaging the human brain with light," J Cereb Blood Flow Metab, 23(1), 1-18 (2003).
[18] M. A. Franceschini, S. Fantini, J. H. Thompson *et al.*, "Hemodynamic evoked response of the sensorimotor cortex measured noninvasively with near-infrared optical imaging," Psychophysiology, 40(4), 548-60 (2003).
[19] R. Kurth, K. Villringer, G. Curio *et al.*, "fMRI shows multiple somatotopic digit representations in human primary somatosensory cortex," Neuroreport, 11(7), 1487-91 (2000).
[20] J. A. Maldjian, A. Gottschalk, R. S. Patel *et al.*, "The sensory somatotopic map of the human hand demonstrated at 4 Tesla," Neuroimage, 10(1), 55-62 (1999).
[21] J. Ruben, J. Schwiemann, M. Deuchert *et al.*, "Somatotopic organization of human secondary somatosensory cortex," Cereb Cortex, 11(5), 463-73 (2001).
[22] R. M. Sanchez-Panchuelo, S. Francis, R. Bowtell *et al.*, "Mapping human somatosensory cortex in individual subjects with 7T functional MRI," J Neurophysiol, 103(5), 2544-56 (2010).
[23] A. K. Singh, M. Okamoto, H. Dan *et al.*, "Spatial registration of multichannel multi-subject fNIRS data to MNI space without MRI," Neuroimage, 27(4), 842-51 (2005).
[24] A. Custo, D. A. Boas, D. Tsuzuki *et al.*, "Anatomical atlas-guided diffuse optical tomography of brain activation," Neuroimage, 49(1), 561-7 (2010).